J Mater Sci (2007) 42:3388–3397
DOI 10.1007/s10853-006-1475-8

The processing of ultrafine-grained materials through the application of severe plastic deformation

Terence G. Langdon

Received: 14 November 2006 / Accepted: 21 December 2006 / Published online: 24 April 2007

Abstract The application of severe plastic deformation (SPD) to bulk metals provides the opportunity of achieving grain sizes in the submicrometer and nanometer range. Several different SPD processing techniques are now available including Equal-Channel Angular Pressing (ECAP), High-Pressure Torsion (HPT) and Accumulative Roll-Bonding (ARB). This paper examines the principles of grain refinement using ECAP and gives examples of the advantageous properties that may be achieved including increased strength at ambient temperatures and a superplastic forming capability at elevated temperatures.

Introduction

It is well known that the mechanical properties of bulk polycrystalline metals depend critically upon the internal microstructural characteristics and especially upon the grain size. If the grain size of a solid is reduced, it is reasonable to anticipate the material will become stronger at ambient temperatures through the Hall–Petch relationship [1, 2]. In addition, since the rate of flow in superplastic deformation varies inversely with the grain size raised to a power of two [3], it is apparent that a reduction in grain size may provide an opportunity for achieving a superplastic forming capability at elevated temperatures. Both of these trends demonstrate significant advantages in preparing materials with very fine grain sizes.

In industrial practice, the grain sizes of commercial alloys are generally reduced through the implementation of appropriate thermo-mechanical processing involving selected regimes of heating and straining that are predetermined independently for each alloy system. However, these procedures lead to grain sizes that are typically no smaller than a few micrometers and it is generally impossible, for all metallic alloy systems, to attain equiaxed grains having sizes lying within the submicrometer (0.1–1.0 μm) or nanometer (<100 nm) ranges. This deficiency means there is a considerable interest in developing new and alternative processing methods that are capable of producing ultrafine-grained materials with grain sizes less than 1 μm.

Two different and complementary approaches may be employed to produce materials with ultrafine grain sizes [4]. The first is the so-called ''bottom-up'' approach in which the solids are assembled from individual atoms as in inert gas condensation [5] or from nanoparticles as in ball-milling with subsequent consolidation [6]. However, it is difficult or impossible to scale these techniques for the production of large bulk solids and, in addition, the materials produced using these procedures invariably contain some degree of residual porosity. The second is the so-called ''top-down'' approach in which a bulk fully-dense solid with a relatively coarse grain size is

Invited paper presented in Symposium C at 5th Brazilian MRS Meeting, Florianópolis, Brazil.

T. G. Langdon (✉)
Department of Aerospace & Mechanical Engineering, University of Southern California, Los Angeles, CA 90089-1453, USA
e-mail: langdon@usc.edu

T. G. Langdon
Department of Materials Science, University of Southern California, Los Angeles, CA 90089-1453, USA

T. G. Langdon
Materials Research Group, School of Engineering Sciences, University of Southampton, Southampton SO17 1BJ, UK

processed to produce an ultrafine-grained material through the application of some form of intense straining.

The principles of using severe plastic deformation (SPD) for the production of strong materials has a long history dating back to the Bai-Lian steels of ancient China [7], the wootz steels of ancient India [8] and the Damascus steels of the Middle East [9]. Nevertheless, it was only in the early 1990's that publications first appeared in the western literature demonstrating that the use of SPD processing provided the capability of producing bulk solids with fairly homogeneous and equiaxed microstructures having grain sizes lying in the submicrometer or nanometer ranges [10, 11]. These reports led to the development of a worldwide interest in the processing and properties of materials processed using various SPD techniques.

Processing by SPD has been defined formally as any method of metal forming under an extensive hydrostatic pressure that may be used to impose a very high strain on a bulk solid without the introduction of any significant change in the overall dimensions of the sample and having the ability to produce exceptional grain refinement [12]. Several different SPD processing techniques are now available including Equal-Channel Angular Pressing (ECAP) [13], High-Pressure Torsion (HPT) [14], Multi-Directional Forging (MDF) [15], Accumulative Roll-Bonding (ARB) [16] and Twist Extrusion (TE) [17]. However, ECAP is an especially attractive process because it can be easily implemented in a materials laboratory using a hydraulic press or a high-capacity mechanical testing facility and, in addition, it can be scaled-up relatively easily for the processing of large bulk samples [18, 19]. Because of these advantages, this paper will deal exclusively with the production of ultrafine-grained materials using ECAP. The following section provides a formal definition of ECAP processing and the subsequent sections describe the application of ECAP to single crystals and polycrystalline materials and give examples of the results that may be achieved through this type of processing.

The principles of ECAP

A detailed description of ECAP is given elsewhere [20] and the principles of the process are illustrated in Fig. 1 [21]. A die is fabricated either from a solid block of tool steel or in the form of two or more plates bolted together. A channel is contained within the die such that the channel has the same cross-sectional dimensions along its length. The channel is bent through an abrupt angle within the die where this angle is generally designated Φ: thus, $\Phi = 90°$ in Fig. 1. The sample is machined to fit within the channel and it is then pressed through the die using a plunger. Shearing occurs when the sample passes through the theoretical shear plane which delineates the plane of intersection between the two separate parts of the channel. As shown in Fig. 1 with reference to the pressed sample, *X*, *Y* and *Z* are used to denote the transverse, flow and longitudinal planes, respectively.

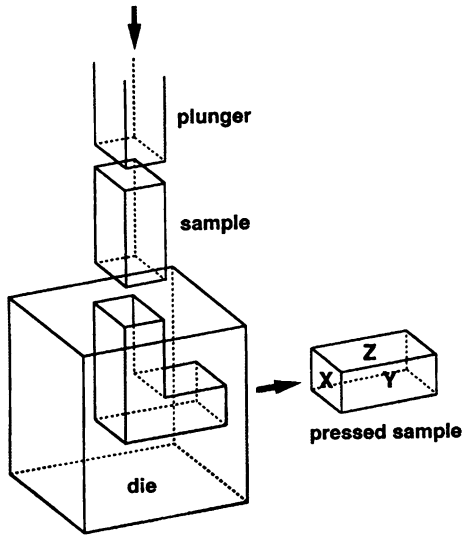

Fig. 1 The principles of ECAP showing the three orthogonal planes *X*, *Y* and *Z* [21]

It can be shown from first principles that the strain imposed on the sample in the passage through the die depends primarily upon the value of Φ and also to a lesser extent upon the value of an angle Ψ representing the outer arc of curvature where the two parts of the channel intersect. In practice, it is apparent that $\Psi = 0°$ in Fig. 1 because the two parts of the channel meet at an abrupt corner without the presence of any arc of curvature. For a die having a channel angle of $\Phi = 90°$, the imposed strain is ~1 for a single pass and this strain varies only to a small extent depending upon the precise value of Ψ [22]. Furthermore, since the cross-sectional dimension of the sample remains unchanged when it passes through the die, it is feasible to repetitively press the same sample in order to impose very high total strains.

When a specimen is pressed repetitively through an ECAP die, different slip systems may be activated by rotating the sample between consecutive passes [23]. Four separate processing routes have been developed and these are designated route A where the sample is not rotated between passes, route B_A where the sample is rotated by 90° in alternate directions between each pass, route B_C where the sample is rotated by 90° in the same direction between each pass and route C where the sample is rotated by 180° between passes [24]. The different shearing planes associated with these different processing routes were described in an earlier report [25] and the shearing patterns were developed in detail for the pressing of bulk and plate

samples [26]. Detailed experiments have shown that an optimum microstructure of equiaxed grains, with a high fraction of high-angle grain boundaries, is achieved most readily when using processing route B_C [27]. There are also additional experiments showing that an optimum microstructure is attained when a high strain is imposed in each separate pass [28], thereby demonstrating that it is preferable to conduct the ECAP processing using a die having a channel angle close to 90°.

The application of ECAP to pure aluminum

Pure aluminum is a convenient model material for investigating the characteristics of the microstructures produced by ECAP. Following the conclusions discussed in the preceding section, all of the results presented in this and subsequent sections relate to processing using an ECAP die with a channel angle of $\Phi = 90°$ and with the samples processed using route B_C whenever specimens are tested through more than one pass.

It is convenient to separately consider the microstructures produced in Al single crystals and in polycrystalline Al. The testing of single crystals is advantageous because it is possible to orient each crystal with respect to both the pressing direction and the theoretical shear plane, thereby providing direct information on the crystallographic nature of the as-pressed microstructures.

Processing by ECAP of Al single crystals

Several investigations have been reported where processing by ECAP has been applied to single crystals: these data include the processing of both aluminum [29–31] and copper [32–35] single crystals. It is convenient to consider tests conducted on single crystals of aluminum where the orientations of the crystals are defined by the schematic illustration in Fig. 2 [29] and the *X*, *Y*, and *Z* orthogonal axes are defined as given earlier in Fig. 1. It is apparent from inspection of Fig. 2 that the theoretical shear plane lies at 45° to the *X* direction. A single crystal may be oriented prior to pressing as shown in the upper part of the entrance channel where the {111} slip plane lies parallel to the theoretical shear plane, the $<110>$ slip direction lies parallel to the direction of shear as the crystal passes through the die and the $<112>$ direction therefore corresponds to the *Y* direction. As illustrated in Fig. 2, this is designated the 0° orientation.

Experiments were conducted on single crystals of aluminum using a die with $\Phi = 90°$ and $\Psi \approx 30°$ and with the crystals oriented either in the 0° orientation as illustrated in Fig. 2 [29] or in orientations where the $\{111\}$ slip plane and the $<110>$ slip direction were rotated about the *Y* axis either in a counter-clockwise sense by 20° to give the –20° orientation [30] or in a clockwise sense by 20° to give the 20° orientation [31]. Of these three different crystallographic orientations, it is especially significant to consider the experiments conducted using the 20° orientation because, since the ECAP die has an arc of curvature of $\Psi \approx 30°$, the slip plane of the primary slip system is then almost coincident with the outer extremity of the shear zone created by the arc of curvature. This close coincidence is illustrated schematically in Fig. 3 where the shear zone is shown shaded and extends through angular increments of ±15° on either side of the theoretical shear plane [31].

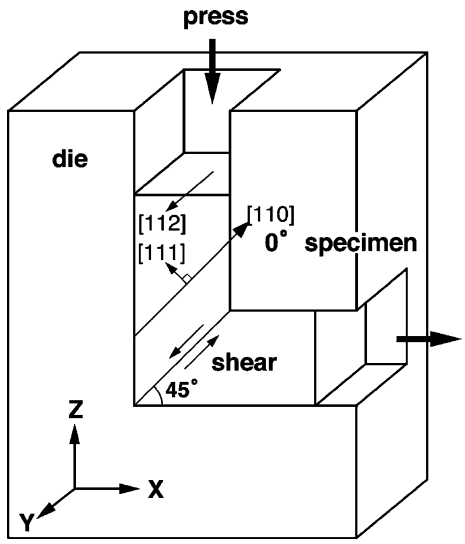

Fig. 2 Section through an ECAP die showing the three orthogonal axes and the characteristics of a single crystal in the 0° orientation [29]

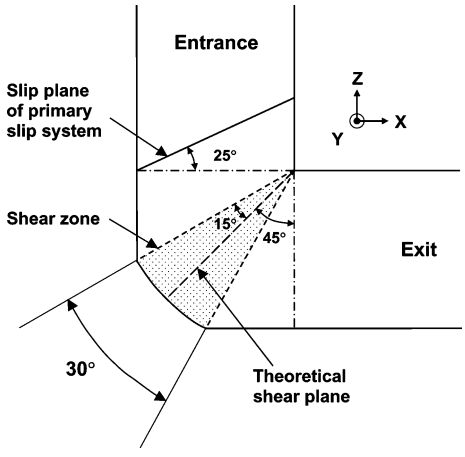

Fig. 3 Schematic illustration on the *Y* plane showing the shear zone associated with an angle of curvature of $\Psi = 30°$ in the ECAP die and the effect of testing a single crystal in a 20° orientation [31]

A single crystal of aluminum in an initial 20° orientation was pressed through a die for one pass and Fig. 4 shows the microstructure visible in the center of the crystal on the *Y* or flow plane together with the corresponding selected area electron diffraction (SAED) pattern: in this illustration, the *X* and *Z* directions lie parallel to the bottom and side edges of the photomicrograph, respectively [31]. Several important conclusions may be reached from inspection of these results. First, the microstructure after a single pass consists of a very well-defined array of elongated cells or subgrains, where the SAED pattern shows these boundaries have low angles of misorientation. Second, these bands are oriented at an angle of approximately 65° with the *X* axis, where this is consistent with the anticipated behavior if the crystal rotates as it passes through the shear zone shown in Fig. 3. Third, the average width of these cells measured perpendicular to their long axis is ~1.3 μm which, as will be shown in the following section, is equal to the average size of the equiaxed grains produced when polycrystalline aluminum is subjected to a number of passes of ECAP. Fourth, careful observations showed that the long axes of the subgrains lie parallel to the slip traces of the primary $(\bar{1}\bar{1}1)[\bar{1}10]$ slip system. These results provide important information that can be used in interpreting the processing by ECAP of polycrystalline aluminum.

Processing by ECAP of polycrystalline Al

Detailed investigations have been conducted to evaluate the microstructural characteristics of polycrystalline Al processed by ECAP [36, 37]. The experiments were conducted using high-purity aluminum with an initial grain size of ~1 mm and with an ECAP die having a channel angle of $\Phi = 90°$ and an arc of curvature of $\Psi = 20°$.

The microstructures recorded on the *X*, *Y* and *Z* planes after a single pass of ECAP are shown in Fig. 5 together with representative SAED patterns [37]. As in Fig. 4 for a single crystal subjected to 1 pass, the microstructure consists of arrays of elongated cells or subgrains with these arrays oriented essentially horizontally when viewed on the *X* plane, at approximately 45° to the *X* axis when viewed on the *Y* plane and perpendicular to the direction of flow when viewed on the *Z* plane. Furthermore, as also observed with the aluminum single crystal, the SAED patterns confirm these boundaries have low angles of misorientation. Finally, it is important to note that the orientations of the arrays visible in Fig. 5 are in excellent agreement with the predictions from detailed theoretical analyses of the shearing patterns produced in ECAP [26].

A more complete understanding of the microstructural refinement produced in ECAP may be obtained by continuing the processing to larger numbers of passes. Examples are shown in Figs. 6 and 7 for polycrystalline Al pressed through 2 and 4 passes, respectively, where the

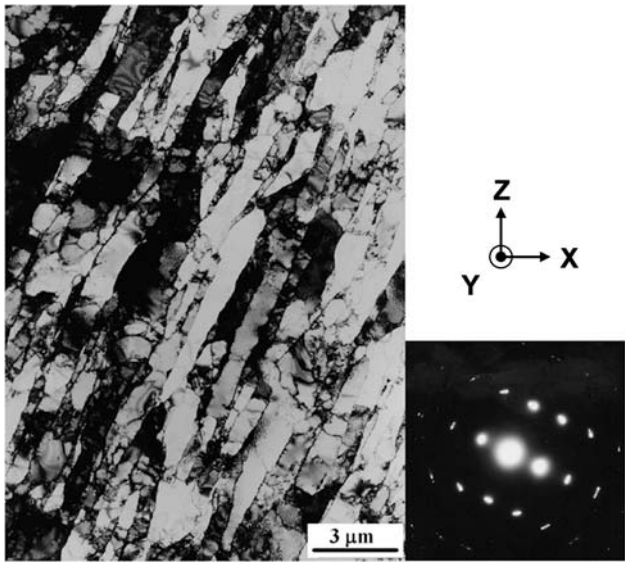

Fig. 4 Microstructure on the *Y* plane in a single crystal of aluminum tested in an initial 20° orientation for one pass and the corresponding SAED pattern [31]

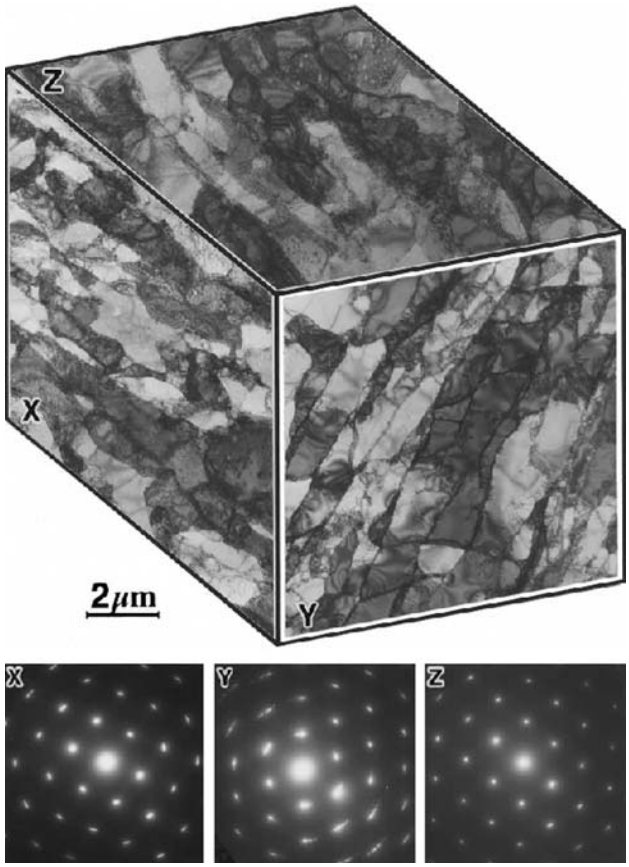

Fig. 5 Microstructures in polycrystalline aluminum on the *X*, *Y* and *Z* planes after one pass and the associated SAED patterns [37]

individual microstructures labeled (a), (b) and (c) correspond to processing using routes A, B_C and C, respectively, and the corresponding SAED patterns are shown below each cube [37]. A careful comparison shows that the microstructures visible in Fig. 6 are fully consistent with the expectations arising from the predicted shearing patterns [26]. For example, the shearing patterns for processing using route C show that shearing is restricted solely to parallel planes oriented at 45° to the *X* axis when viewed on the *Y* plane whereas the shearing lies horizontally when viewed on the *X* plane and vertically, or perpendicular to the flow direction, when viewed on the *Z* plane [26]: all of these predictions match the microscopic evidence visible in Fig. 6(c). There is also a similar agreement between predictions and experiments when processing using routes A and B_C.

The situation is different after 4 passes of ECAP as shown in Fig. 7 because in this condition the microstructures on the three orthogonal planes for route B_C, shown in Fig. 7b, are reasonable homogeneous with arrays of essentially equiaxed grains and, based on the SAED patterns, a high fraction of boundaries having high angles of misorientation. More recent experiments on high purity polycrystalline Al using orientation imaging microscopy have confirmed these trends [38, 39]. By contrast, it is apparent from Fig. 7a and c that the subgrains remain elongated after processing through 4 passes using routes A and C and the SAED patterns show these microstructures contain a high fraction of low-angle boundaries.

An important result from the microstructures developed using route B_C is that the average size of the subgrains, on each of the orthogonal planes of sectioning, is in the range of ~1.2–1.3 μm. Since this is similar to the average width of the subgrain arrays formed on a single pass in the Al single crystal, as shown in Fig. 4, it is reasonable to conclude that the equilibrium grain size attained in processing by ECAP is determined by the average width of the subgrain arrays developed in the first pass. An additional important conclusion from inspection of Fig. 7b is that the microstructures after 4 passes are essentially identical on each plane of sectioning and accordingly the grain size of the pure Al has been effectively reduced from an initial value of ~1 mm to a final value of ~1.3 μm through the simple procedure of pressing for 4 passes using route B_C

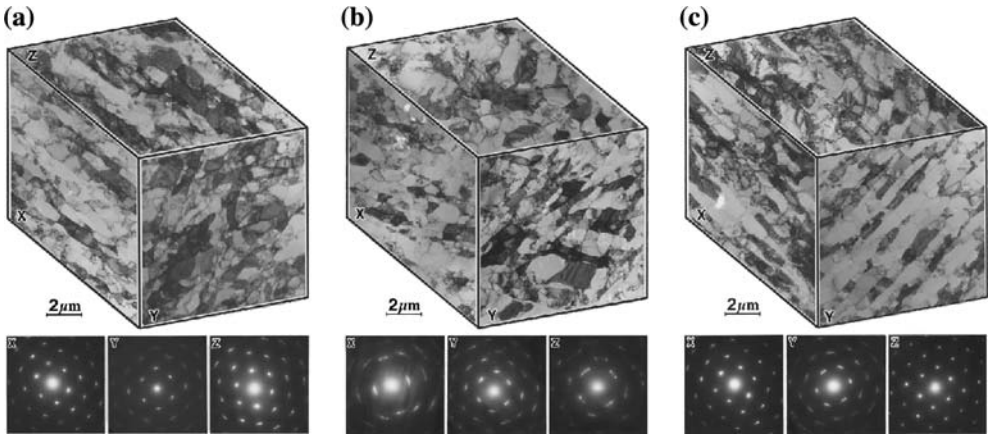

Fig. 6 Microstructures in polycrystalline aluminum on the *X*, *Y* and *Z* planes after two passes for processing using (**a**) route A, (**b**) route B_C and (**c**) route C and the associated SAED patterns [37]

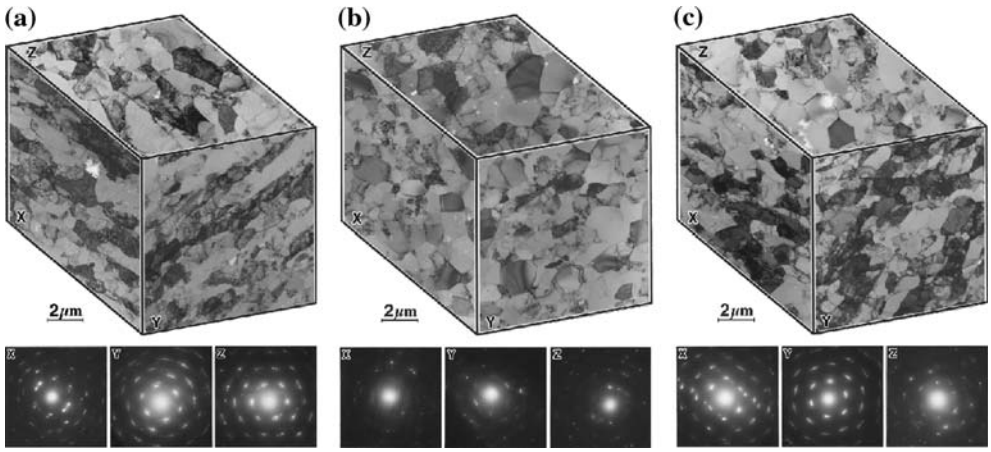

Fig. 7 Microstructures in polycrystalline aluminum on the *X*, *Y* and *Z* planes after four passes for processing using (**a**) route A, (**b**) route B_C and (**c**) route C and the associated SAED patterns [37]

with an ECAP die having a channel angle of 90°. Finally, there is evidence that the equilibrium grain size produced in ECAP is essentially identical to the subgrain size achieved in conventional cold-working operations such as compression or extrusion [40].

Principles of grain refinement in ECAP

The experimental microstructures recorded for pure Al have been used to develop a simple model for grain refinement during ECAP [41]. This model is shown in Fig. 8 where the microstructures are shown after the first pass in row 1, after 2 passes in row 2 and after 4 passes in row 3, the separate columns for 2 and 4 passes relate to processing using routes A, B_C and C, respectively, and, based on the analyses of shearing patterns [26], the value of η below each illustration denotes the predicted total angular range for the various slip systems operating up to and including that particular pass. Thus, the subgrain array visible on the *Y* plane after the first pass in the top row is consistent both with the microstructural appearance for a single crystal in Fig. 4 and with a polycrystalline sample in Fig. 5. For convenience, the average width of these subgrains is denoted as *d*. For 2 passes, row 2 denotes the slip systems operating in the first and second pass for each processing route, with total angular ranges of 27°, 18° and 0° for routes A, B_C and C, respectively. Finally, for 4 passes in the bottom row the angular ranges become 37°, 63° and 0° for routes A, B_C and C, respectively. Again, each pass introduces an array of cells or subgrains with an average width of *d*.

It is apparent from Fig. 8 that there is a high total angular range for slip of 63° after processing through 4 passes using route B_C. This gives rise to the presence of numerous intersecting slip systems and accordingly it is reasonable to anticipate the very high density of dislocations will re-arrange and annihilate in a manner consistent with the Low-Energy Dislocation Structures (LEDS) theory [42, 43]. Thus, this will lead to an array of reasonably equiaxed grains on each orthogonal plane of sectioning after 4 passes using route B_C whereas the development of an equiaxed array will proceed more slowly when using routes A and C because of the lower values for the total angular range of slip.

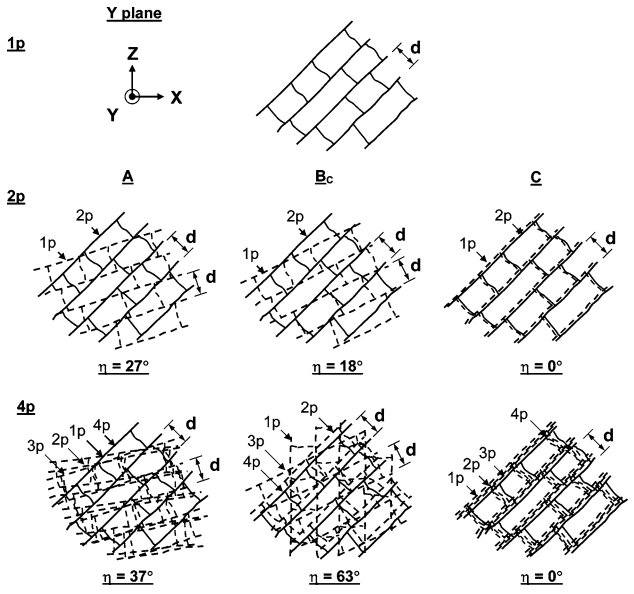

Fig. 8 A model for grain refinement in ECAP showing the microstructural development on the *Y* plane after 1 pass in the top row, 2 passes in the second row and 4 passes in the third row: the three columns for 2 and 4 passes denote the slip systems that are present when using processing routes A, B_C and C, respectively [41]

Properties achieved after processing by ECAP

Mechanical properties at ambient temperature

The introduction of significant grain refinement through processing by ECAP suggests that these ultrafine-grained materials will exhibit high strength. This is confirmed in Fig. 9 which shows the 0.2% proof stress measured in tension at room temperature for a series of commercial alloys subjected to ECAP using route B_C and a die with a channel angle of $\Phi = 90°$ [44]. Since the channel angle was 90°, it follows that equivalent strains of 1, 2, 4 and 6 correspond to 1, 2, 4 and 6 passes through the die, respectively. It is apparent from Fig. 9 that the 0.2% proof stress increases for each alloy by a factor of between two

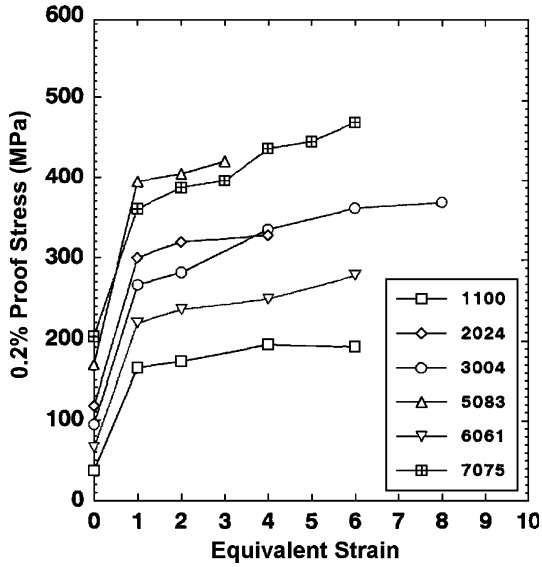

Fig. 9 Values of the 0.2% proof stress versus the equivalent strain for several commercial aluminum alloys processed by ECAP [44]

and three on the first pass through the die but thereafter there is only a rather minor increase. These results demonstrate, therefore, that the additional strengthening is introduced primarily in the first pass. For all of the alloys listed in Fig. 9, observations by transmission electron microscopy showed that the grain sizes were within the submicrometer range after processing by ECAP.

Mechanical properties at elevated temperatures

Superplasticity may be achieved at elevated temperatures in materials having small grain sizes and it is now well-established that the flow rate within the superplastic regime varies inversely with the grain size raised to a power of two [3]. This means in practice that a reduction in grain size by one order of magnitude will increase the superplastic strain rate by two orders of magnitude and accordingly it led to the suggestion that the ultrafine-grained materials achieved by ECAP should exhibit superplastic elongations, and therefore a superplastic forming capability, at exceptionally rapid strain rates [45]. It is not feasible in practice to attain good superplastic ductilities in pure metals or solid solution alloys processed by ECAP because, as demonstrated in static annealing experiments [46], the grains grow rapidly when these materials are heated to the elevated temperatures required for superplastic flow. Accordingly, it is necessary to use materials where precipitates are present to inhibit grain growth. This effect was first demonstrated using an Al–Mg–Li–Zr alloy and an Al–Cu–Zr alloy [47] where exceptional superplastic elongations were achieved at strain rates at and above 10^{-2} s^{-1} within the regime generally termed high strain rate superplasticity [48].

An example of exceptional superplasticity after processing by ECAP is shown in Fig. 10 for an Al–3% Mg–0.2% Sc alloy processed through 8 passes using route B_C in a die with a channel angle of $\Phi = 90°$ [49]. The open points in Fig. 10 show tensile data recorded after pressing for tests conducted at temperatures in the range from 573 to 723 K. Inspection shows this alloy exhibits exceptionally high elongations, up to and above 2000%, at testing strain rates above 10^{-2} s^{-1}. Furthermore, these elongations cannot be achieved using conventional cold rolling as shown by the solid points labeled C.R. where the material was cold-rolled at room temperature without ECAP and then tested in tension at 673 K. These results demonstrate conclusively both the advantageous properties that may be attained using processing by ECAP and the inability to achieve similar properties using more conventional processing. A second example is shown in Fig. 11 where a commercial Al–Mg–Li–Zr alloy was processed using route B_C and a die with $\Phi = 90°$ either for 4 passes at 673 K in Fig. 11a or for 8 passes at 673 K and an additional 4 passes at 473 K in

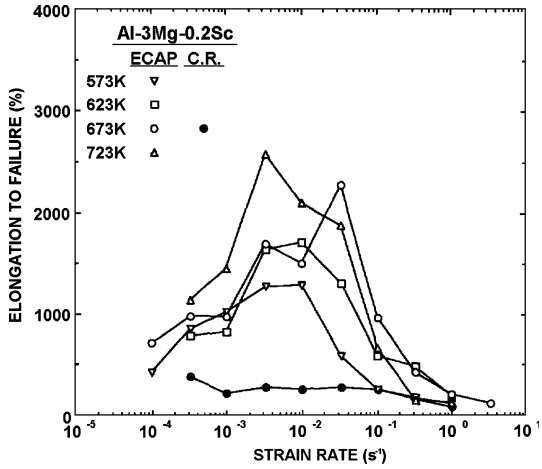

Fig. 10 Elongation to failure versus testing strain rate for an Al–3% Mg–0.2% Sc alloy processed by ECAP: data are shown also for the same alloy processed by cold rolling (C.R.) without ECAP [49]

Fig. 11b [50]. These results show not only that the alloy exhibits exceptional ductilities after ECAP but also that the peak elongations are displaced to faster strain rates when there is an increase in the total strain imposed in ECAP. The solid points shown near the bottom of both plots denote the results from testing the non-superplastic alloy in the as-received condition.

The high elongations achieved in these materials in tensile testing after processing by ECAP suggests that the pressed alloys should form easily under an external pressure. This may be checked for the Al–3% Mg–0.2% Sc alloy by cutting disks from the as-pressed billets, inserting into a biaxial gas-pressure forming facility, heating to a representative temperature such as 673 K were the material exhibits excellent properties as shown in Fig. 10 and then subjecting the disks, on one side only, to a constant pressure of argon gas for very short periods of time. Examples are shown in Fig. 12 where the forming was achieved through the application of a gas pressure of 10 atmospheres, equivalent to 1 MPa, at 673 K in a die-less facility: it should be noted that the disk on the left at (a) is untested and the other disks were held under a constant gas pressure for times of (b) 30 s and (c) 60 s [51]. The easy forming of these domes in an alloy that is nominally not superplastic confirms the excellent superplastic forming capability that may be introduced through ECAP processing. Furthermore, sectioning of the domes and careful measurements showed the alloy has an exceptionally high thinning factor of ~0.85–0.89 where the thinning factor denotes the ratio of the measured thickness at any point on the dome to the average thickness assuming constant volume and uniform deformation [52]. This high degree of uniformity in forming after ECAP is due to the exceptionally small submicrometer grain size that is introduced in the alloy during the pressing operation.

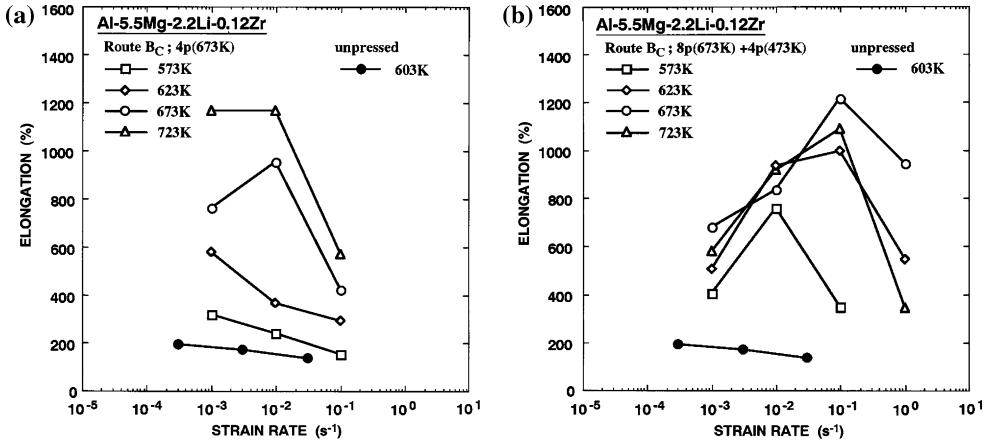

Fig. 11 Elongation to failure versus strain rate for an Al–Mg–Li–Zr alloy processed (**a**) for 4 passes at 673 K and (**b**) for 8 passes at 673 K and an additional 4 passes at 473 K: the lower solid points show data for the unpressed alloy [50]

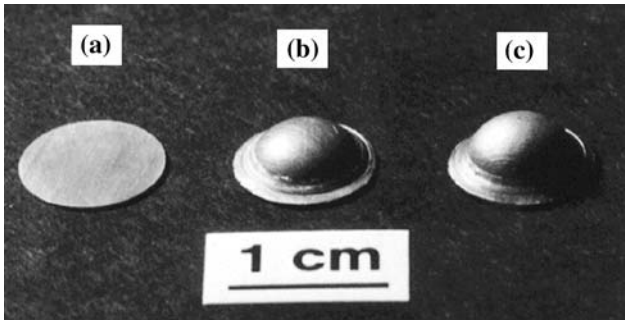

Fig. 12 Examples of the superplastic forming of an Al–3% Mg–0.2% Sc alloy processed by ECAP and subjected to a gas pressure of 10 atmospheres at 673 K: (**a**) an untested disk after ECAP, (**b**) a disk held at pressure for 30 s and (**c**) a disk held at pressure for 60 s [51]

Discussion

Processing by ECAP provides an opportunity for producing very significant grain refinement, typically to the submicrometer level, with the consequent development of superior mechanical properties that cannot be achieved using conventional processing techniques. Although 'The application of ECAP to pure aluminum' of this report refers specifically to the application of ECAP to samples of pure aluminum where this is taken as a representative model material, in practice processing by ECAP has been applied to a very wide range of materials including two-phase alloys such as the Ti–6% Al–4% V alloy [53], multi-phase alloys such as the magnetic Pr_{20}–$Fe_{73.5}B_5Cu_{1.5}$ alloy [54], eutectoid alloys such as Zn–22% Al [55–57] and metal matrix composites such as the Al-6061 alloy reinforced with 10 vol% Al_2O_3 particles [58–60].

It is generally true that processing by ECAP leads to a strengthening of the alloy at ambient temperature through the Hall–Petch relationship [1, 2] as shown in Fig. 9 but nevertheless it is important to recognize that the pressing operation may also introduce a weakening effect. An example of weakening is provided by very recent work on a spray-cast Al-7034 alloy where pressing at a temperature of 473 K gave a weakened material by comparison with the as-received alloy [61]. This result was due to the high pressure imposed in ECAP on the precipitates contained within the matrix. For example, careful inspection showed that pressing of the Al-7034 alloy at a temperature of 473 K led both to a fragmentation of the long rod-like η-phase of $MgZn_2$ [61, 62] and, as a consequence of the high dislocation density, to a concurrent precipitation of the η-phase [63].

The potential for developing superplastic forming capabilities through ECAP processing is described in 'Mechanical properties at elevated temperatures'. In practice, there are now numerous reports describing superplastic behavior in materials processed by ECAP and a very recent review provides a detailed tabulation of these data [64]. When conventional materials deform in the superplastic regime, it is known that failure often occurs through the nucleation, growth and coalescence of internal cavities [65]. Only very limited data are at present available documenting the occurrence of cavitation in the tensile testing of materials processed by ECAP [66]. However, since an understanding of the failure processes of bulk ultrafine-grained materials is an important requirement if these materials are to find use in industrial applications, it seems likely that this will become an important area for future investigations.

Summary and conclusions

1. Processing by equal-channel angular pressing (ECAP) is now well-established as a procedure for achieving grain refinement to at least the submicrometer level in a range of polycrystalline metals. Extensive experiments using pure aluminum as a model material, in both single crystal and polycrystalline form, have

provided detailed information on the microstructural characteristics of this grain refinement.

2. The materials produced by ECAP processing usually exhibit high strength at ambient temperatures. Experiments show the strength may be weakened by ECAP if, for example, the pressure and temperature of the pressing operation, combined with the very high dislocation density, lead to precipitate fragmentation and additional precipitation.
3. The submicrometer grain sizes attained by ECAP processing are favorable for achieving superplastic flow and a superplastic forming capability at high strain rates. Forming operations show that the exceptionally small grain sizes introduced by ECAP lead to essentially uniform thinning and a very high thinning factor.

Acknowledgements Presentation of this paper at the 5th Brazilian Materials Research Society Meeting in Florianópolis in October 2006 was made possible through support from SBPMat (Sociedade Brasileira de Pesquisa em Materiais). I am grateful to Prof. Levi Bueno (Universidade Federal de São Carlos) for making all travel arrangements within Brazil. This work was supported by the National Science Foundation of the United States under Grant No. DMR-0243331 and the U.S. Army Research Office under Grant No. W911NF-05-1-0046.

References

1. Hall EO (1951) Proc Roy Soc B 54:747
2. Petch NJ (1953) J Iron Steel Inst 174:25
3. Langdon TG (1994) Acta Metall Mater 42:2437
4. Zhu YT, Lowe TC, Langdon TG (2004) Scripta Mater 51:825
5. Gleiter H (1989) Prog Mater Sci 33:223
6. Koch CC, Cho YS (1992) Nanostruct Mater 1:207
7. Wang JT (2006) Mater Sci Forum 503–504:363
8. Srinivasan S, Ranganathan S (2004) India's legendary wootz steel: an advanced material of the ancient world. National Institute of Advanced Studies and Indian Institute of Science, Bangalore, India
9. Sherby OD, Wadsworth J (2001) J Mater Proc Technol 117:347
10. Valiev RZ, Krasilnikov NA, Tsenev NK (1991) Mater Sci Eng A137:35
11. Valiev RZ, Korznikov AV, Mulyukov RR (1993) Mater Sci Eng A168:141
12. Valiev RZ, Estrin Y, Horita Z, Langdon TG, Zehetbauer MJ, Zhu YT (2006) JOM 58(4):33
13. Segal VM, Reznikov VI, Drobyshevskiy AE, Kopylov VI (1981) Russian Metall 1:99
14. Smirnova NA, Levit VI, Pilyugin VI, Kuznetsov RI, Davydova LS, Sazonova VA (1986) Fiz Metal Metalloved 61:1170
15. Salishchev GA, Valiahmetov OR, Galeev RM (1993) J Mater Sci 28:2898, DOI: 10.1007/BF00354692
16. Saito Y, Tsuji N, Utsunomiya H, Sakai T, Hong RG (1998) Scripta Mater 39:1221
17. Varyutkhin VN, Beygelzimer YY, Synkov S, Orlov D (2006) Mater Sci Forum 503–504:335
18. Horita Z, Fujinami T, Langdon TG (2001) Mater Sci Eng A318:34
19. Srinivasan R, Cherukuri B, Chaudhury PK (2006) Mater Sci Forum 503–504:371
20. Valiev RZ, Langdon TG (2006) Prog Mater Sci 51:881
21. Berbon PB, Furukawa M, Horita Z, Nemoto M, Langdon TG (1999) Metall Mater Trans 30A:1989
22. Iwahashi Y, Wang J, Horita Z, Nemoto M, Langdon TG (1996) Scripta Mater 35:143
23. Segal VM (1995) Mater Sci Eng A197:157
24. Furukawa M, Iwahashi Y, Horita Z, Nemoto M, Langdon TG (1998) Mater Sci Eng A257:328
25. Furukawa M, Horita Z, Nemoto M, Langdon TG (2001) J Mater Sci 36:2835, DOI: 10.1023/A:1017932417043
26. Furukawa M, Horita Z, Langdon TG (2002) Mater Sci Eng A332:97
27. Oh-ishi K, Horita Z, Furukawa M, Nemoto M, Langdon TG (1998) Metall Mater Trans 29A:2011
28. Nakashima K, Horita Z, Nemoto M, Langdon TG (1998) Acta Mater 46:1589
29. Fukuda Y, Oh-ishi K, Furukawa M, Horita Z, Langdon TG (2004) Acta Mater 52:1387
30. Furukawa M, Kawasaki Y, Miyahara Y, Horita Z, Langdon TG (2005) Mater Sci Eng A410–411:194
31. Fukuda Y, Oh-ishi K, Furukawa M, Horita Z, Langdon TG (2006) Mater Sci Eng A420:79
32. Miyamoto H, Erb U, Koyama T, Mimaki T, Vinogradov A, Hashimoto S (2004) Phil Mag Lett 84:235
33. Miyamoto H, Fushimi J, Mimaki T, Vinogradov A, Hashimoto S (2005) Mater Sci Eng A405:221
34. Furukawa M, Fukuda Y, Oh-ishi K, Horita Z, Langdon TG (2006) Mater Sci Forum 503–504:113
35. Miyamoto H, Fushimi J, Mimaki T, Vinogradov A, Hashimoto S (2006) Mater Sci Forum 503–504:799
36. Iwahashi Y, Horita Z, Nemoto M, Langdon TG (1997) Acta Mater 45:4733
37. Iwahashi Y, Horita Z, Nemoto M, Langdon TG (1998) Acta Mater 46:3317
38. Terhune SD, Swisher DL, Oh-ishi K, Horita Z, Langdon TG, McNelley TR (2002) Metall Mater Trans 33A:2173
39. Salem AA, Langdon TG, McNelley TR, Kalidindi SR, Semiatin SL (2006) Metall Mater Trans 37A:2879
40. Semiatin SL, Berbon PB, Langdon TG (2001) Scripta Mater 44:135
41. Langdon TG (2007) Mater Sci Eng (in press)
42. Kuhlmann-Wilsdorf D (1989) Mater Sci Eng A113:1
43. Kuhlmann-Wilsdorf D (1997) Scripta Mater 36:173
44. Horita Z, Fujinami T, Nemoto M, Langdon TG (2000) Metall Mater Trans 31A:691
45. Ma Y, Furukawa M, Horita Z, Nemoto M, Valiev RZ, Langdon TG (1996) Mater Trans JIM 37:336
46. Hasegawa H, Komura S, Utsunomiya A, Horita Z, Furukawa M, Nemoto M, Langdon TG (1999) Mater Sci Eng A265:188
47. Valiev RZ, Salimonenko DA, Tsenev NK, Berbon PB, Langdon TG (1997) Scripta Mater 37:1945
48. Higashi K, Mabuchi M, Langdon TG (1996) ISIJ Intl 36:1423
49. Komura S, Horita Z, Furukawa M, Nemoto M, Langdon TG (2001) Metall Mater Trans 32A:707
50. Lee S, Berbon PB, Furukawa M, Horita Z, Nemoto M, Tsenev NK, Valiev RZ, Langdon TG (1999) Mater Sci Eng A272:63
51. Horita Z, Furukawa M, Nemoto M, Barnes AJ, Langdon TG (2000) Acta Mater 48:3633
52. Cornfield GC, Johnson RH (1970) Intl J Mech Sci 12:479
53. Semenova IP, Raab GI, Saitova LR, Valiev RZ (2004) Mater Sci Eng A387–389:805
54. Stolyarov VV, Gunderov DV, Popov AG, Puzanova TZ, Raab GI, Yavari AR, Valiev RZ (2002) J Magnetism Magnetic Mater 242–245:1399
55. Furukawa M, Ma Y, Horita Z, Nemoto M, Valiev RZ, Langdon TG (1998) Mater Sci Eng A241:122

56. Huang Y, Langdon TG (2002) J Mater Sci 37:4993, DOI: 10.1023/A:1021071228521
57. Kumar P, Xu C, Langdon TG (2005) Mater Sci Eng A410–411:447
58. Valiev RZ, Islamgaliev RK, Kuzmina NF, Li Y, Langdon TG (1999) Scripta Mater 40:117
59. Li Y, Langdon TG (2000) J Mater Sci 35:1201, DOI: 10.1023/A:1004740504619
60. Kawasaki M, Huang Y, Xu C, Furukawa M, Horita Z, Langdon TG (2005) Mater Sci Eng A410–411:402
61. Xu C, Furukawa M, Horita Z, Langdon TG (2005) Acta Mater 53:749
62. Xu C, Furukawa M, Horita Z, Langdon TG (2003) Acta Mater 51:6139
63. Gao N, Starink MJ, Furukawa M, Horita Z, Xu C, Langdon TG (2005) Mater Sci Eng A410–411:303
64. Kawasaki M, Langdon TG (2007) J Mater Sci 42:1782
65. Langdon TG (1982) Metal Sci 16:175
66. Kawasaki M, Xu C, Langdon TG (2005) Acta Mater 53:5353